

About Detecting Very Low Mass Black Holes in LAr Detectors

Ionel Lazanu,^a Sorina Lazanu,^{b,1} Mihaela Pârnu^a

^aUniversity of Bucharest, Faculty of Physics, POBox MG-11 Bucharest-Magurele, Romania

^bNational Institute of Materials Physics, POBox MG-7 Bucharest-Magurele, Romania

E-mail: ionel.lazanu@g.unibuc.ro, lazanu@infim.ro, mihaela.parvu@unibuc.ro

Abstract. The nature of dark matter is still an open problem. The simplest assumption is that gravity is the only force coupled certainly to dark matter and thus the micro black holes could be a viable candidate. We investigated the possibility of direct detection of micro black holes with masses around and upward the Planck scale (10^{-5} g), ensuring classical gravitational treatment of these objects in the next generation of huge LAr detectors. We show that the signals (ionization and scintillations) produced in LAr enable the discrimination between micro black holes or other particles. It is expected that the trajectories of these micro black holes will appear as crossing the whole active medium, in any direction, producing uniform ionization and scintillation on all the path.

Keywords: dark matter detectors, primordial black holes

¹Corresponding author

Contents

1	Introduction	1
2	Detection mechanisms	2
2.1	Rates	2
2.2	Gravitational, electronic and nuclear energy loss	4
2.3	The electronic stopping powers	4
2.4	The nuclear stopping power	5
3	Production of scintillation light in liquid argon	5
4	Results and discussions	6
5	Summary	11

1 Introduction

There is a general consensus that the observable universe contains 72% dark energy, 24% dark matter and only 4% ordinary matter. Following the arguments of Paul Frampton [1], the only interaction which we know for certain to be experienced by dark matter is gravity and the simplest assumption is that gravity is the only force coupled to dark matter. There is no strong argument that the weak interaction must be automatically considered in dark matter interactions. The possible candidates for dark matter constituents are axions, WIMPs, baryonic MACHOs, neutrino (axino, gravitino), *etc.* The possibility that non-radiating “micro” black holes - μ BH exist should be taken seriously; such black holes could be part of the dark matter in the Universe. Any possibility to observe or to determine observational limits on the number of μ BH (independent of the assumption that they radiate) is very useful.

An important issue is to show that black holes do not radiate in some conditions and which are their characteristics, as an argument to explain that these relics objects can survive from early Universe. We would need to detect the black holes or to have strong indirect evidence of their existence, as well as to show that they do not radiate. At present we are far from doing this.

In a classical paper, Hawking [2] suggested that unidentified tracks in the photographs taken in old bubble chamber detectors could be explained as signals of gravitationally collapsed objects (μ BH). The mechanism of black hole formation is well known. As a result of fluctuations in the early Universe, a large number of gravitationally collapsed objects can be formed with characteristics determined by the gravity and quantum behaviour. For masses above the Planck mass limit of 10^{-5} g quantum behaviour is prevented.

The small black holes are expected to be unstable due to Hawking radiation, but the evaporation is not well-understood at masses of order of the Planck scale. Helfer [3] has shown that none of the derivations that have been given for the prediction of radiation from black holes is convincing. It argued that all involve, at some point, speculations on the physics at scales which are not merely orders of magnitude beyond any investigated experimentally ($\sim 10^3$ GeV), but at scales increasing beyond the Planck scale ($\sim 10^{19}$ GeV), where essentially

quantum-gravitational effects are expected to be dominant and various derivations that have been put forward, not all are mutually consistent.

Given the profound nature of the issues addressed, some disagreement and controversy exists over exactly what has been achieved. Balbinot [4] demonstrated that when a black hole becomes more and more charged, the Hawking radiation decreases and in the limit of maximum charge containment there is no radiation. Certain inflation models naturally assume the formation of a large number of small black hole [5] and the GUP may indeed prevent total evaporation of small black holes by dynamics and not by symmetry, just like the prevention of hydrogen atom from collapse by the standard uncertainty principle [6]. Chavda and Chavda [7] introduced a different idea: gravitationally bound black holes will not have Hawking radiation. They examine the range $10^{-24} \text{ kg} \leq M_{BH} \leq 10^{-12} \text{ kg}$ where quantum aspects must be considered. These limits of masses are controversial regarding the stability of the black holes, see for example [8].

Neutral or charged micro black holes? In the paper of Lehmann and co-workers [9] the authors discuss a possible scenario about the accumulation of electric charge. In this scenario, the black hole evaporates, it emits charged particles of both signs, and it does so stochastically. Thus, during the evaporation process, non-zero electric charges are generated. If evaporation is cut off sharply at some mass scale in the order of M_{Pl} , the black hole might be frozen with leftover electric charge of random sign. Hawking argues that black holes can carry an electric charge $|Z| \leq 30$ in electron units.

Moving in a material medium, depending on the electric charge, these primordial μBH can capture electrons or protons to form neutral "atoms", but also starting from this state the stripping processes can be considered.

A μBH with electric charge is an object able to capture electromagnetically electrons or protons depending on its charge, up to the formation of an atom, and also bounds these particles gravitationally. Ordinary gravitational orbits are in the high quantum number, continuum classical limit. Newtonian gravity is generally valid for $r > 10 R_{BH}$ since the difference between Einstein's general relativity and Newtonian gravitation gets small in this region. Using the prescription of Rabinowitz, pages 38-40 from reference [8], the gravitational binding energy of a proton is $E_b^{grav} \approx 23.5 \text{ MeV}$ and for the electron the value is decreased with the ratio between masses, respectively.

In this paper we present arguments in favour of the possibility of direct detection of such μBH in LAr detectors, based on their interactions in the material of the target.

2 Detection mechanisms

2.1 Rates

Recent estimates from global methods for dark matter densities lie in the range $(0.2 - 0.6) \text{ GeV/cm}^3$. A major source of uncertainty is the contribution of baryons (stars, gas, and stellar remnants) to the local dynamical mass. New studies of the local DM density from Gaia satellite data yield $(0.4 - 1.5) \text{ GeV/cm}^3$, depending on the type of stars used in the study. An updated halo model predicts values of $(0.55 \pm 0.17) \text{ GeV/cm}^3$, where the 30% error accounts for the systematics [10]. Other observational quantities of interest are the local circular speed v_c and the escape velocity v_{esc} . The obtained values are $v_c = (218 - 246) \text{ km/s}$ and $v_{esc} = 533_{-41}^{+54} \text{ km/s}$ [10]. We expect these very low mass objects to have velocities in the range from 250 km/s up to 1000 km/s because their primary motion is under the effect of the gravity.

Detector	Reference	Technology	Active Mass of Argon
DarkSide	[12]	Dual-Phase	33 kg
ArDM	[13]	Dual-Phase	850 kg
MiniCLEAN	[14]	Single-Phase	500 kg
DEAP	[15]	Single-Phase	3600 kg
ArgoNeuT	[16]	Single-Phase	0.02 ton
MicroBooNE	[17]	Single-Phase	170 ton
ICARUS	[18]	Single-Phase	600 ton
ProtoDUNE-SP	[19]	Single-Phase	770 ton
ProtoDUNE-DP	[20]	Dual-Phase	760 ton
DUNE	[21]	Single+Dual-Phase	up to 4×10 kton

Table 1: Current Ar experiments and future projects.

In the hypothesis that the single components of the dark matter are the μ BH objects, the flux can be calculated as:

$$\Phi_{\mu BH} \cong \frac{\rho_{DM}}{M_{\mu BH}} v_{DM} \cong 1.6 \times [10^{-16} \div 10^{-35}] \text{ part}/(\text{m}^2\text{s}). \quad (2.1)$$

where: $\rho_{DM}=0.35 \text{ GeV}/\text{cm}^3$, $v_{DM}=250 \text{ km}/\text{s}$ and $M_{\mu BH}=[10^{-5} \div 10^{14}] \text{ g}$.

The interaction of the neutral black hole atoms with ordinary matter via the gravitational dynamical friction effect is extremely weak, as it was first shown in [5]. This is due to the extremely small cross-section, in the order of $\sim \pi r_g^2 \times (c/v)^2 \sim 3 \times 10^{-60} \text{ m}^2$ [11].

In very simplified approximation, the total rate R (no correction considered) is equal to

$$R = \text{flux} \times \text{number of target particles} \times \text{cross section}. \quad (2.2)$$

In accordance with Hawking [2], for elastic collisions of neutral black hole atoms, the cross section is in the order of 10^{-20} m^2 for an electronic atom and 10^{-27} m^2 for a protonic one. The number of target particles (N_t) is calculated as: $N_t = N_A \frac{M_t}{A}$ where N_A is Avogadro's number, (A , M_t) are the mass number and mass of the target (detector). Thus the rate of events is:

$$R [\text{part./year}] = 7.6 \times M_t [\text{kg}] \times \begin{cases} 10^{-48} \text{ gravitational interaction} \\ 10^{-8} \text{ elastic; for "electronic atom"} \\ 10^{-15} \text{ elastic; for "protonic atom"} \end{cases} \quad (2.3)$$

where the last column is the multiplicative factor considering the gravitational interaction, elastic scattering for the "electronic atom" and the "protonic atom" respectively.

In Table 1 we present a compilation of the current experiments and future projects on neutrino physics that are able to detect these objects.

For many of these experiments, the target masses are insufficient to achieve realistic interaction rates. In these very rough estimations, around 3 events/ year are expected for the DUNE detector with all 4 modules.

2.2 Gravitational, electronic and nuclear energy loss

When a projectile interacts with Ar, it loses energy by gravitational interactions, and/or transfers energy to atomic electrons producing ionizations and excitations, and/or interact elastically directly with nuclei as Coulomb processes.

The gravitational effects in the transmission of μBH through matter can be estimated in the classical impulse approximation using the analogy with the Bohr formalism for ions. The μBH energy loss per unit length is

$$\frac{dE}{dx} = \frac{4\pi G^2 M^2 \rho}{v^2} \ln\left(\frac{b_{max}}{b_{min}}\right) \sim \frac{4\pi G^2 M^2 \rho}{v^2} \times (10 \div 30). \quad (2.4)$$

where G is Newton's constant, $\rho = m \times n$ is the mass density of the target particles with n the number density of the target particles. The term $\ln\left(\frac{b_{max}}{b_{min}}\right)$ changes weakly for a very large domain of impact parameters due to the logarithmic dependence. A value between 10 and 30 was suggested by Rabinowitz [8].

At very low energies, the interaction of the μBH with nuclei gets dominant compared with the contribution of the interaction with electrons. In the second step, recoil nuclei interact also with electrons and other nuclei up to their stopping in LAr and the energy transferred can be neglected.

Electronic and nuclear stopping powers are calculated using the procedure used by Lazanu and Lazanu in previous papers [22, 23]. The energy transferred in electronic processes is used for ionization and for excitation of the electrons.

In fact, one can consider the LAr as consisting of two subsystems: electronic and nuclear. The energy lost by the projectile is partitioned between these subsystems, which have different energy distributions, equivalent with two different temperatures. For a transient period of time a transfer of energy between subsystems must be considered simultaneously with the diffusion of heat in space.

In this case the primary interaction in LAr, seen as binary process, takes place under the condition $M \gg m_i$, with $i = \text{Ar}, e$; in both cases the maximum transferred energy is $E_{K, max} \cong 2m_i c^2 \beta^2 \gamma^2$.

For velocities of μBH of 250÷1000 km/s, the kinetic energy transferred in an interaction to electrons is of the order 1÷10 eV and (51.7÷827.2) keV to argon nuclei respectively. Ionization potential in the liquid phase is 13.4 eV. The average energy required to produce an electron-ion pair in LAr is $W_i = 23.6 \pm 0.3$ eV, a value that is smaller than that obtained in gaseous argon $W_g = 26.4$ eV. In these circumstances μBH s have a small contribution to excitation and ionization processes, while nuclear processes are dominant.

2.3 The electronic stopping powers

In this low energy range of the μBH of interest here, the electronic stopping of the charged incoming particle in the target is treated within the local density approximation; the ion-target interaction is treated as that of a particle with a density averaged free electron gas. The basic assumptions of this approximation are: a) the electron density in the target varies slowly with position. b) available electron energy levels and transition strengths are described by those in a free electron gas and there are no significant band-gap effects. c) the charge of the ion can be reduced to a scalar quantity called the ion's effective charge.

The concrete procedure to define the effective charge of the ion is through the square of the ratio between the stopping power of the ion and the stopping power of hydrogen, while

the effective charge of the hydrogen depends also on the kinetic energy and projectile mass [24].

At low energies, Lindhard's formula [25] is used, where the energy loss is proportional to the velocity.

The electronic (masic) stopping power is

$$S_{el}(E) = \frac{1}{\rho} \times \left(\frac{dE}{dx} \right)_{el} = 2.307 \times 10^9 \times \frac{Z^{7/6} Z_{Ar}}{\left(Z^{2/3} + Z_{Ar}^{2/3} \right)^{3/2}} \times \frac{1}{A_{Ar}} \times \left(\frac{E}{A} \right)^{1/2}. \quad (2.5)$$

in units of [eV \times cm²/g]. In this equation E is given in keV, A in atomic mass units, and Z is the effective charge of the μ BH.

At high energies, if the velocity of projectile is $v > v_{Bohr}$ of electrons in atom, the electronic stopping power is calculated using Bethe-Bloch formula. Due to their intrinsic neutrality, WIMPs do not interact directly with electrons; they can interact as a singular process with nuclei, and ionizations and excitations are only produced by the recoil nuclei. μ BHs, even if at a certain moment could be neutral protonic or electronic atoms, capture or stripping reactions take place and thus, μ BHs will interact in matter by Coulomb interactions.

2.4 The nuclear stopping power

The nuclear stopping power is calculated using Ziegler, Biesack, Litmark formalism [26]. The reduced energy ε is defined as:

$$\varepsilon = \frac{32.53 A_{Ar}}{A + A_{Ar}} \times \frac{E}{Z Z_{Ar} \left(Z^{2/3} + Z_{Ar}^{2/3} \right)^{1/2}}. \quad (2.6)$$

where the energy E is expressed in keV. Correspondingly, the reduced nuclear stopping cross section:

$$S_n(\varepsilon) = \frac{1}{2} \frac{\ln(1 + \varepsilon)}{\varepsilon + 0.10718 \varepsilon^{0.37544}}. \quad (2.7)$$

With these definitions, the nuclear masic stopping power is:

$$S_{nucl}(E) = \frac{1}{\rho} \times \left(\frac{dE}{dx} \right)_{nucl} = 5.097 \times 10^9 \frac{Z Z_{Ar}}{(A + A_{Ar}) \left(Z^{2/3} + Z_{Ar}^{2/3} \right)^{1/2}} \times \frac{A}{A_{Ar}} \times S_n(\varepsilon) \quad (2.8)$$

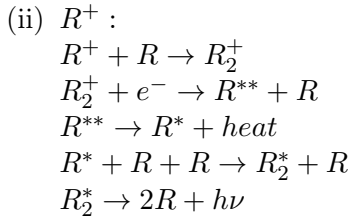
in units of [eV \times cm²/g]. In the first step, when the μ BH interacts directly in the detector, the charge and mass numbers are $Z \rightarrow Z_{\mu BH}$ (effective charge) and $A \rightarrow A_{\mu BH}$; in all the other cases, the projectile is the Ar self-recoil so $Z \rightarrow Z_{Ar}$ (effective charge) and $A \rightarrow A_{Ar}$.

For charged μ BH and for ions moving in matter, in the calculus of electronic stopping their effective charge must be considered and this value varies with the velocity.

3 Production of scintillation light in liquid argon

Following the model of Doke and co-workers [27], in argon, two distinct ways as possible for scintillations:

- (i) R^* :
- $$R^* + R + R \rightarrow R_2^* + R$$
- $$R_2^* \rightarrow 2R + h\nu$$



In processes (i) and (ii), the excited dimer at the lowest excited level should be de-excited to the dissociative ground state by emitting a single UV photon, because the energy gap between the lowest excitation level and the ground level is so large that there exists no decay channel such as nonradiative transitions. Although this is not yet fully confirmed by experiments, authors assume that each excited dimer emits a single photon.

After the interaction of the incident particle, singlet and triplet dimers will be produced, and the scintillation is a product of the two radiative decays following the excitation process. Liquid and gaseous argon are transparent to its own scintillation light. In the case of double phase technology, ionizations and scintillations are produced in both phases. In accordance with [30], the singlet decays quickly, being responsible for most of the prompt light seen in the scintillation spectrum, whereas the triplet decays with a longer lifetime. The time constants of the singlet and triplet decays have been measured in all phases and their lifetimes, both in ns, are: 7.0 ± 1.0 and 1600 ± 100 respectively. The existence of different impurities in argon put in evidence the differences in the emission spectra of liquid and gaseous phases [28, 29]. In LAr, the spectrum is dominated by an emission feature 126.8 nm or 9.78 keV equivalent value analogues to the 2nd excimer continuum in the gas phase [31], confirming the previous results of Doke [27]. Weak-emission features in the wavelength range from 145 to 300 nm were observed. The structure at 155 nm in the gas phase has only a very weak analogue in the liquid phase. The structure at longer wavelengths up to 320 nm is addressed as the 3rd continuum emission in the gas phase.

Inspired by Refs. [32] and [33] the response of LAr to electronic excitation is presented in Figure 1. Recently, in different and successive experiments, the ionization yield of nuclear recoils in LAr have been measured in the lower energy range: at 6.7 keV [34], 17 - 57 keV [35] and at higher energies, at 80 and 233 keV [36]. These measurements cover part of the energy range of interest for the present study. Because the present analysis is not dedicated to the detection possibilities specific to a particular experiment, we will make only a few general considerations. The S1 and S2 light yields depend on the strength of electric field in drift interaction region, mainly due to recombination effect of ionizing electrons. Unfortunately, the basic properties of S1 and S2 of argon are not well known. Recently, Washimi and co-workers [37, 38] focused their studies on the drift-field dependence of S2/S1 properties for the interval 0.2 - 3.0 kV/cm, of interest for two-phase argon detectors. In figure 2 from reference [38] the drift field dependences of S1 and S2 signals are presented, as well as the S2/S1 ratio properties with a two-phase detector at drift-fields [37].

4 Results and discussions

The gravitational energy loss for a μBH of 10^{-5} g mass and 250 km/s velocity, evaluated using eq. (4) is in the order 0.9×10^{-21} keV cm²/g, and in the next discussion it will be neglected in respect to the electronic and nuclear energy loss.

In Figure 2 we present the velocity dependence of the nuclear and electronic energy loss in LAr for the μBH and for Ar recoils produced in the interaction of the μBH in the detector.

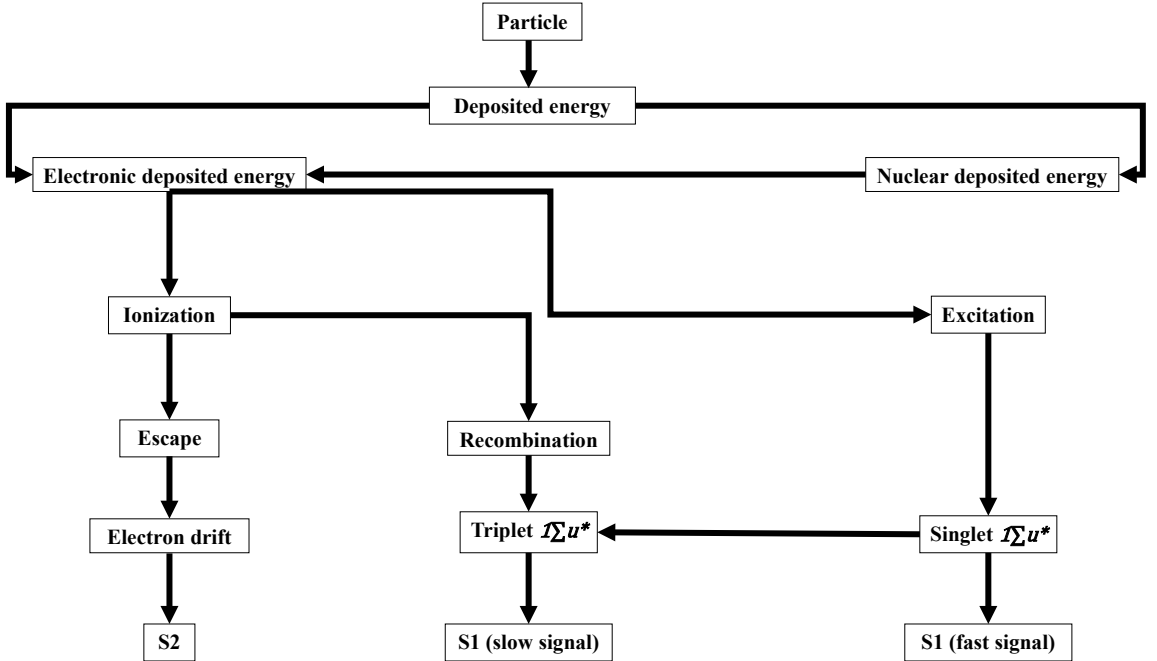


Figure 1: The liquid argon response to interaction of incident charged particle.

As we specified earlier, for WIMPs interactions there is no electronic energy loss produced, but only that due to recoil-induced processes. For comparison with the μBH , the energy loss of a heavy ion (uranium was considered as example) in LAr is also included in the figure, at the same velocities, allowing to highlight the differences expected in the signals resulting from the interactions. One can see that the U ion has higher energy loss than the μBH , both nuclear and electronic. The energy loss for the μBH was calculated using eqs. 2.5 and 2.6, while the values for Ar and U are from SRIM [39]. The results put clearly in evidence the peculiarities of the energy losses of μBH s both in electronic and nuclear processes, compared with Ar self-recoils and with uranium ions. For μBH and for U ions in LAr, the nuclear energy loss is greater than the electronic energy loss in the range of velocities investigated. For recoil Ar nuclei, the electronic energy loss is greater above 1200 km/s.

Transient thermal processes follow the scattering process, when an appreciable amount of energy is released in a small region of a material, and in a very short time interval. There are more models in the literature for these processes, one of them being the thermal spike. In this model, there are two subsystems, namely electrons and nuclei, which are coupled through the energy transfer, which could take place in both directions.

Heat diffusion in both subsystems is described by the classical heat equation, supposing the existence of two sources: one source is given by the energy released through electronic energy loss, the other by nuclear energy loss. The consideration of two sources is compulsory in the regime of comparable electronic and nuclear energy losses. This thermodynamic model is not the most appropriate way to follow, but the only one for which the formalism allows an unambiguous approach. A detailed description of the model, equations and steps to solve the time and space evolution of both subsystems is discussed in reference [40]. Nuclear energy

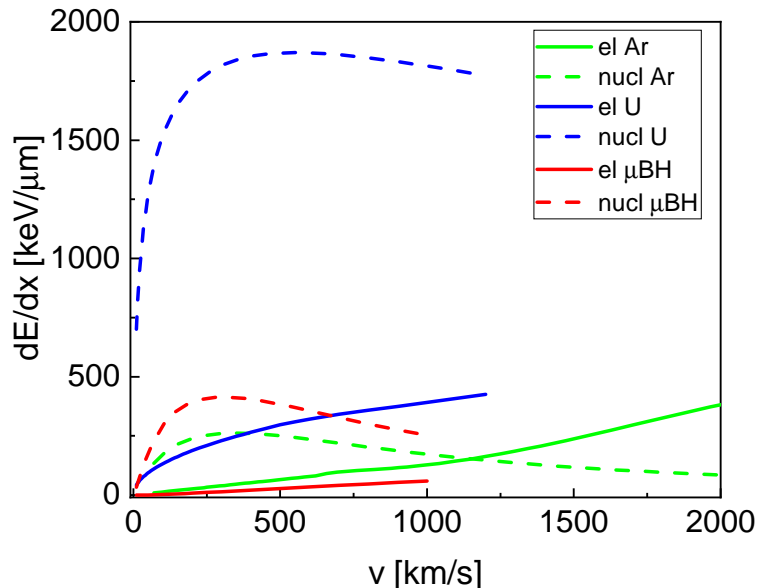


Figure 2: Electronic (lines) and nuclear (dashed lines) energy loss for the μ BH, Ar selfrecoils and U ions in LAr.

loss is dominant at the end of range, or at low kinetic energies, while the electronic stopping becomes more and more important at high energies. Both recoils and secondary electrons produce heating effects in spreading their energy.

The thermal spike model was developed initially by Koehler and Seitz [41] for effects produced by irradiation in crystals and by Seitz to explain bubble formation due to charged particles interacting in liquids [42]. Toulemonde *et al.* [43] have applied the thermal spike model to water. The electronic and atomic (or molecular) sub-systems in the LAr target have different temperatures, and are coupled through a term proportional to the temperature difference between them. The energy depositions around the trajectories of ions in fluids were modelled as thermal spikes and pressure waves using the equations of fluids dynamics by Apfel *et al.* [44]; in this model, only the energy transferred to the atomic system is considered by the authors, the electronic component being neglected. We use here the model of the thermal spike. The dependence of the temperatures of electron and molecular subsystems on the distance to the track of the projectile (recoil), r , and on the time after its passage, t , are solutions of two coupled partial differential equations [23]:

$$\begin{aligned} C_e(T_e) \frac{\partial T_e}{\partial t} &= \frac{1}{r} \frac{\partial}{\partial r} \left[r K_e(T_e) \frac{\partial T_e}{\partial r} \right] - g(T_e - T_{mol}) + A(r, t) \\ C_{mol}(T_{mol}) \frac{\partial T_{mol}}{\partial t} &= \frac{1}{r} \frac{\partial}{\partial r} \left[r K_{mol}(T_{mol}) \frac{\partial T_{mol}}{\partial r} \right] - g(T_{mol} - T_e) + B(r, t) \end{aligned} \quad (4.1)$$

where $T_{e(mol)}$, $C_{e(mol)}$, and $K_{e(mol)}$ are respectively the temperatures, the specific heat, and the thermal conductivities of the electronic (index e) and molecular subsystems (index mol).

The sources satisfy the conservation laws:

$$\begin{aligned} \int_0^\infty dt \int_0^\infty 2\pi r A(r, t) dr &= \left(\frac{dE}{dx} \right)_{el} \\ \int_0^\infty dt \int_0^\infty 2\pi r B(r, t) dr &= \left(\frac{dE}{dx} \right)_n \end{aligned} \quad (4.2)$$

with $\left(\frac{dE}{dx} \right)_{el}$ and $\left(\frac{dE}{dx} \right)_n$ the electronic and nuclear linear energy losses, respectively. While the thermodynamic parameters for LAr were extensively investigated, the ones corresponding to

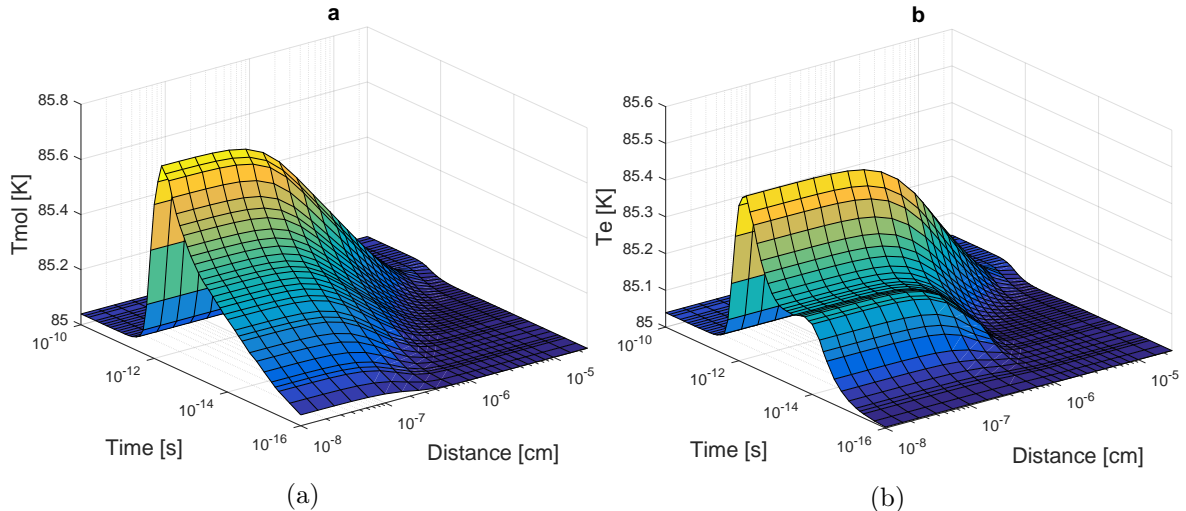


Figure 3: Time and space variation of the temperature of the molecular (a) and electronic system (b) in LAr produced by a μBH of 250 km/s velocity, 10^{-5} g mass and 30 charge number.

the electronic subsystem are not known. In the numerical calculations, the values of C_{mol} and K_{mol} for LAr were taken from [45], while for the electronic one the values from Ref. [41] were used. For the coupling constant between the sub-systems, related to the mean free path of electrons, a value of 10^{13} W cm $^{-3}$ K $^{-1}$ was taken.

In LAr, it is generally agreed that the energy deposited into the electronic subsystem is divided between ionization and scintillation, 82.6% and 17.4% respectively. Supposing that the applied electric field directs the electrons to the electrode, we assume that only the part not assigned to ionization from the electronic energy loss is available for energy exchange with the molecular subsystem.

In Fig. 3a and 3b the development of the thermal spike in space and time is illustrated. It is produced by a μBH of 10^{-5} g mass and 250 km/s velocity. The electronic and molecular subsystems have different characteristic times, *i.e.* 5×10^{-15} and 5×10^{-13} s respectively. One can see a small increase of the electronic temperature due to the electronic energy loss, and another increase due to the transfer from the atomic (molecular) subsystem.

These results highlight the following aspects of the temporal and spatial evolution of transient phenomena: a) at a time scale of the order of 10^{-16} s and a spatial scale of atomic dimensions, the two subsystems receive energy by transfer from the projectile in accordance with linear energy losses, and keeping into account that only part of the energy transferred to electronic sub-system is available for exchange; b) at a time scale of the order 5×10^{-13} s, the atomic subsystem dominantly transfers energy to the electronic one, which uses it to produce additional ionizations and excitations. In the case of μBH this is the dominant component of ionization and excitation energy; c) in these processes, the temperature increase does not produce liquid-gas phase transition for an initial temperature of LAr of 85 K.

The thermal spike produced by an Ar self-recoil of 300 keV kinetic energy, produced by the collision with the μBH of 250 km/s velocity and 10^{-5} g mass at maximum transferred energy is represented in Fig. 4a and 4b.

The main difference in respect to the thermal spike produced by the μBH consists in the fact that for the Ar selfrecoil the electronic energy loss is higher, and it produces the

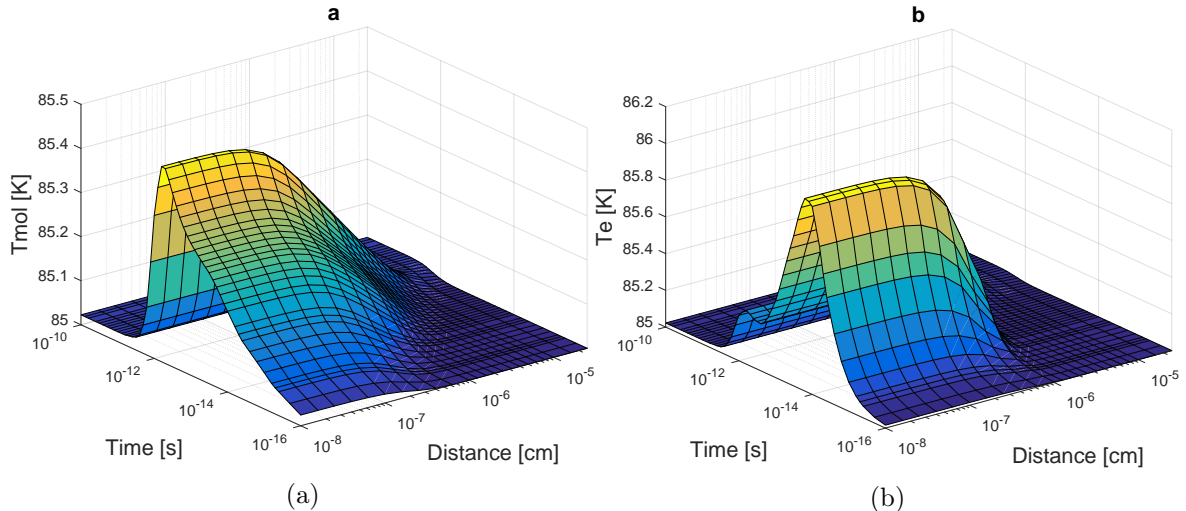


Figure 4: Time and space variation of the temperature of the molecular (a) and electronic system (b) of LAr produced by an Ar selfrecoil of 50 keV kinetic energy, resulting from the interaction of a μBH of velocity 250 km/s, mass 10^{-5} g and charge number 30 with an Ar nucleus, at maximum energy transfer.

most important peak in the electronic temperature at times characteristic to the electronic sub-system, while the peak corresponding to the transfer for the molecular sub-system is comparatively lower.

The energy transferred from the molecular to the electronic subsystem on unit range has been calculated [37] as:

$$\left(\frac{dE}{dx}\right)_{ex} = \int_0^\infty dt \int_0^\infty 2\pi r g (T_{mol} - T_e) dr. \quad (4.3)$$

In Figure 5 we present the energy transferred by the molecular system to the electronic one in LAr for the μBH , and for Ar selfrecoils. In all cases, the transfer direction is the same, *i.e.* the electronic subsystem receives energy in transient processes in the investigated range of velocities. These transferred energies modify significantly the initial Lindhard partition of the energy loss.

The maximum absolute scintillation yield is defined by the average energy (W') to produce a single photon. For calculation, Doke *et al.* [46] defined a practical quantity, as: $W_{ph}(\text{max}) = W/(1 + N_{ex}/N_i)$, where W is the average energy required to form an ion-electron pair. For argon $W_{ph}(\text{max}) = 19.5 \pm 1.0\text{eV}$ [27].

Although the energy lost by the μBH during its passage through LAr is negligible in respect to its energy, the energy deposited in the electronic subsystem produces ionizations and excitations that are at the base of its detection.

Thus, for a μBH of velocity 250 km/s and 10^{-5} g mass, our calculations revealed that, following the transfer of energy from the molecular subsystem, $(dE/dx)_{el}$ is 60 keV/ μm . The average energy transferred to an Ar recoil in a head-in collision is 25 keV, and in its turn it eventually losses 76 keV/ μm as excitations and ionizations, considering also the transfer from the molecular subsystem. In this conditions 6.97×10^3 photons/ μm are estimated and

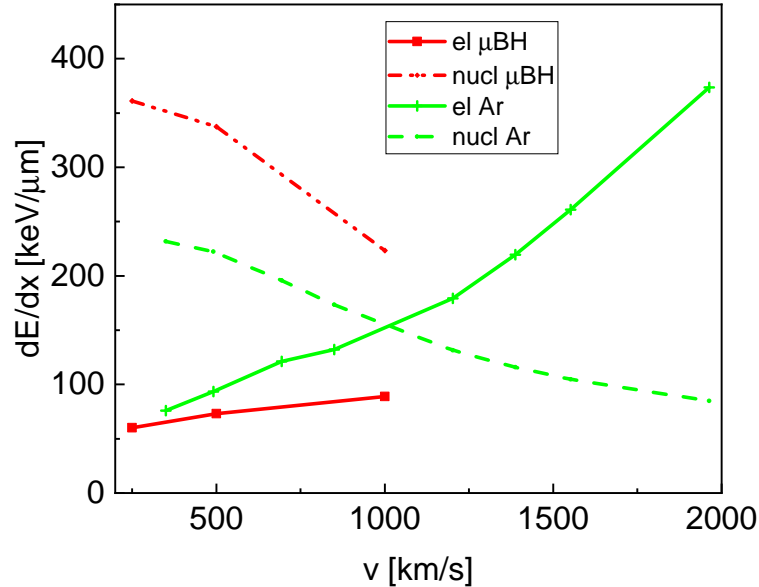


Figure 5: Electronic (lines) and nuclear (dashed lines) energy loss for the μBH and Ar selfrecoils in liquid Ar after the exchange of energy from nuclear to electronic subsystem.

this maximal component will contribute to scintillations.

Consequently, in the analysis of tracks in LAr detectors, the trajectories of these μBH will appear as crossing the whole active medium, in any direction, producing uniform ionization and scintillation for all the path.

5 Summary

We investigated the possibility of direct detection of hypothetical objects formed just in the very early time after the Big Bang, and which survived until now. We considered the case of black holes with masses around and upward the Planck scale (10^{-5} g) which ensure classical gravitational treatment of the objects. The μBH are viable candidates in explaining the nature of dark matter. Originally proposed by Stephen Hawking in 1971, in recent years these objects became an important option especially when other highly sought-after candidates have not been discovered. In this work, using the initial idea of their existence, we considered that such relics carry electric charges up to 30 in units of e . We discussed some arguments in favour of the supposition that they do not radiate and thus they have survived until now. The results obtained for their electronic and nuclear stopping powers in LAr, calculated in the frame of the Lindhard and Ziegler formalism with consideration of the transient processes treated in the frame of the thermal spike model, with the consideration of the transfer of energy between electronic and molecular subsystems, open the possibility of their direct detection in future generation of huge LAr detectors. The main uncertainty for more realistic predictions is the flux of these objects. Our estimations show that the discrimination between the signals (ionization and scintillations) produced by these μBH and other heavy ions or other particles is possible. There is a clear distinction between expected signals from μBH objects and WIMPs for example.

Acknowledgments

IL and MP acknowledge the support from the Romanian Programme PNCDI III, CERN-RO, under Contract 2/2019.

References

- [1] P. H. Frampton, “Primordial Intermediate Mass Black Holes as Dark Matter,” [[arXiv:2004.10540](https://arxiv.org/abs/2004.10540) [astro-ph.GA]].
- [2] S. Hawking, “Gravitationally collapsed objects of very low mass,” *Mon. Not. Roy. Astron. Soc.* **152**, 75 (1971), <https://doi.org/10.1093/mnras/152.1.75>
- [3] A. D. Helfer, “Do black holes radiate?,” *Rept. Prog. Phys.* **66**, 943-1008 (2003) doi:10.1088/0034-4885/66/6/202 [[arXiv:gr-qc/0304042](https://arxiv.org/abs/gr-qc/0304042) [gr-qc]].
- [4] R. Balbinot, “NEGATIVE ENERGY RADIATION FROM A CHARGED BLACK HOLE,” *Class. Quant. Grav.* **3**, L107-L110 (1986) doi:10.1088/0264-9381/3/5/003
- [5] P. Chen, “Inflation induced Planck-size black hole remnants as dark matter,” *New Astron. Rev.* **49**, 233-239 (2005) doi:10.1016/j.newar.2005.01.015 [[arXiv:astro-ph/0406514](https://arxiv.org/abs/astro-ph/0406514) [astro-ph]].
- [6] R. J. Adler, P. Chen and D. I. Santiago, “The Generalized uncertainty principle and black hole remnants,” *Gen. Rel. Grav.* **33**, 2101-2108 (2001) doi:10.1023/A:1015281430411 [[arXiv:gr-qc/0106080](https://arxiv.org/abs/gr-qc/0106080) [gr-qc]].
- [7] L. Chavda and A. L. Chavda, “Dark matter and stable bound states of primordial black holes,” *Class. Quant. Grav.* **19**, 2927 (2002) doi:10.1088/0264-9381/19/11/311 [[arXiv:gr-qc/0308054](https://arxiv.org/abs/gr-qc/0308054) [gr-qc]].
- [8] M. Rabinowitz, “Little black holes as dark matter candidates with feasible cosmic and terrestrial interactions,” [[arXiv:physics/0503079](https://arxiv.org/abs/physics/0503079) [physics]].
- [9] B. V. Lehmann, C. Johnson, S. Profumo and T. Schwemberger, “Direct detection of primordial black hole relics as dark matter,” *JCAP* **10**, 046 (2019) doi:10.1088/1475-7516/2019/10/046 [[arXiv:1906.06348](https://arxiv.org/abs/1906.06348) [hep-ph]].
- [10] M. Tanabashi et al. (Particle Data Group), *Phys. Rev. D* **98**, 030001 (2018).
- [11] V. Dokuchaev and Y. N. Eroshenko, “Black hole atom as a dark matter particle candidate,” *Adv. High Energy Phys.* **2014**, 434539 (2014) doi:10.1155/2014/434539 [[arXiv:1403.1375](https://arxiv.org/abs/1403.1375) [astro-ph.CO]].
- [12] <http://darkside.lngs.infn.it/>
- [13] <http://darkmatter.ethz.ch/>
- [14] <http://deapclean.org/>
- [15] <http://deap3600.ca/>.
- [16] <https://t962.fnal.gov/>.
- [17] https://microboone.fnal.gov.
- [18] https://icarus.fnal.gov.
- [19] <https://home.cern/>.
- [20] <https://home.cern/deap>.
- [21] B. Abi *et al.* [DUNE], “Deep Underground Neutrino Experiment (DUNE), Far Detector Technical Design Report, Volume I Introduction to DUNE,” [[arXiv:2002.02967](https://arxiv.org/abs/2002.02967) [physics.ins-det]].

- [22] I. Lazanu and S. Lazanu, “Interactions of exotic particles with ordinary matter,” Nucl. Instrum. Meth. B **278**, 70-77 (2012) doi:10.1016/j.nimb.2012.02.008 [arXiv:1111.1984 [astro-ph.IM]].
- [23] I. Lazanu and S. Lazanu, “Transient thermal effects in solid noble gases as materials for the detection of Dark Matter,” JCAP **07**, 013 (2011) doi:10.1088/1475-7516/2011/07/013 [arXiv:1103.1841 [astro-ph.IM]].
- [24] Ziegler, J.F. Handbook of stopping cross-sections for energetic ions in all elements, United States: Pergamon Press Incorporated (1980).
- [25] Lindhard, J, Scharff, M, and Schioett, H E. RANGE CONCEPTS AND HEAVY ION RANGES (NOTES ON ATOMIC COLLISIONS, II) N. p., 1963, <https://www.osti.gov/biblio/4153115-range-concepts-heavy-ion-ranges-notes-atomic-collisions-ii>.
- [26] Biersack J.P., Ziegler J.F. (1982) The Stopping and Range of Ions in Solids. In: Ryssel H., Glawischnig H. (eds) Ion Implantation Techniques. Springer Series in Electrophysics, vol 10. Springer, Berlin, Heidelberg, ISBN="978-3-642-68779-2"
- [27] T. Doke, A. Hitachi, J. Kikuchi, K. Masuda, H. Okada and E. Shibamura, “Absolute Scintillation Yields in Liquid Argon and Xenon for Various Particles,” Jap. J. Appl. Phys. **41**, 1538-1545 (2002) doi:10.1143/JJAP.41.1538
- [28] A. Buzulutskov, “Photon emission and atomic collision processes in two-phase argon doped with xenon and nitrogen,” EPL **117**, no.3, 39002 (2017) doi:10.1209/0295-5075/117/39002 [arXiv:1702.03612 [physics.ins-det]].
- [29] T. Heindl, T. Dandl, M. Hofmann, R. Krucken, L. Oberauer, W. Potzel, J. Wieser and A. Ulrich, “The scintillation of liquid argon,” EPL **91**, no.6, 62002 (2010) doi:10.1209/0295-5075/91/62002 [arXiv:1511.07718 [physics.ins-det]].
- [30] A. Hitachi, T. Takahashi, N. Funayama, K. Masuda, J. Kikuchi and T. Doke, “Effect of ionization density on the time dependence of luminescence from liquid argon and xenon,” Phys. Rev. B **27**, 5279-5285 (1983) doi:10.1103/PhysRevB.27.5279
- [31] M. PÁĕrvu and I. Lazanu, “Short analysis of cosmogenic production of radioactive isotopes in argon as target for the next neutrino experiments”, Radiat. Phys. Chem. **152**, 129 (2018) doi:10.1016/j.radphyschem.2018.08.009.
- [32] Masayo Suzuki, Jian-zhi Ruan(Gen), Shinzou Kubota, Time dependence of the recombination luminescence from high-pressure argon, krypton and xenon excited by alpha particles, Nuclear Instruments and Methods in Physics Research, Volume 192, Issues 2&A3, 1982, [https://doi.org/10.1016/0029-554X\(82\)90874-6](https://doi.org/10.1016/0029-554X(82)90874-6)
- [33] M. Kimura, M. Tanaka and K. Yorita, “Low Energy Response on Liquid Argon Scintillation and Ionization Process for Dark Matter Search,” JPS Conf. Proc. **11**, 040003 (2016) doi:10.7566/JPSCP.11.040003
- [34] T. Joshi, S. Sangiorgio, A. Bernstein, M. Foxe, C. Hagmann, I. Jovanovic, K. Kazkaz, V. Mozin, E. Norman, S. Pereverzev, F. Rebassoo and P. Sorensen, “First measurement of the ionization yield of nuclear recoils in liquid argon,” Phys. Rev. Lett. **112**, 171303 (2014) doi:10.1103/PhysRevLett.112.171303 [arXiv:1402.2037 [physics.ins-det]].
- [35] H. Cao *et al.* [SCENE], “Measurement of Scintillation and Ionization Yield and Scintillation Pulse Shape from Nuclear Recoils in Liquid Argon,” Phys. Rev. D **91**, 092007 (2015) doi:10.1103/PhysRevD.91.092007 [arXiv:1406.4825 [physics.ins-det]].
- [36] A. Bondar, A. Buzulutskov, A. Dolgov, E. Grishnyaev, S. Polosatkin, L. Shekhtman, E. Shemyakina and A. Sokolov, “Measurement of the ionization yield of nuclear recoils in liquid argon at 80 and 233 keV,” EPL **108**, no.1, 12001 (2014) doi:10.1209/0295-5075/108/12001 [arXiv:1407.7348 [physics.ins-det]].

- [37] T. Washimi, M. Kimura, M. Tanaka and K. Yorita, “Scintillation and ionization ratio of liquid argon for electronic and nuclear recoils at drift-fields up to 3 kV/cm,” *Nucl. Instrum. Meth. A* **910**, 22-25 (2018) doi:10.1016/j.nima.2018.09.019 [[arXiv:1805.06367](#) [[physics.ins-det](#)]].
- [38] T. Washimi, T. Kikuchi, M. Kimura, M. Tanaka and K. Yorita, “Study of the low-energy ER/NR discrimination and its electric-field dependence with liquid argon,” *JINST* **13**, no.02, C02026 (2018) doi:10.1088/1748-0221/13/02/C02026
- [39] Ziegler, J.F., Ziegler, M.D., and Biersack, J.P.: 2010, *Nuclear Instruments and Methods in Physics Research B* **268**, [10.1016/j.nimb.2010.02.091](#)
- [40] I. Lazanu and S. Lazanu, “Contribution of the electron-phonon interaction to Lindhard energy partition at low energy in Ge and Si detectors for astroparticle physics applications,” *Astropart. Phys.* **75**, 44-54 (2016) doi:10.1016/j.astropartphys.2015.09.007 [[arXiv:1505.06340](#) [[astro-ph.IM](#)]].
- [41] Koehler, J.S., and Seitz, F.: 1954, “Radiation Disarrangement of Crystals,” *Zeitschrift fur Physik* **138**, 238, DOI:[10.1007/BF01340667](#).
- [42] F. Seitz, “On the Theory of the Bubble Chamber,” *Phys. Fluids* **1**, no.1, 2-13 (1958) doi:[10.1063/1.1724333](#)
- [43] M. Toulemonde, E. Surdutovich and A.V. Solovyov, Temperature and pressure spikes in ion-beam cancer therapy, *Phys. Rev. E* **80** (2009), doi:[10.1103/PhysRevE.80.031913](#)
- [44] Apfel RE, Sun YY, Nath R. Transient thermal and mechanical response of water subject to ionizing radiation. *Radiat Res.* 1992;131(2):124-132, doi:[10.2307/3578432](#)
- [45] E. Aprile, A. E. Bolotnikov, A. L. Bolozdynya and T. Doke, “Noble Gas Detectors,” doi:[10.1002/9783527610020](#)
- [46] T. Doke, H. Crawford, A. Hitachi, J. Kikuchi, P. Lindstrom, K. Masuda, E. Shibamura and T. Takahashi, “Let Dependence of Scintillation Yields in Liquid Argon,” *Nucl. Instrum. Meth. A* **269**, 291-296 (1988) doi:[10.1016/0168-9002\(88\)90892-3](#)